Sensitivity in Detecting Osseous Lesions Depends on Anatomic Localization: Planar Bone Scintigraphy Versus ^{18}F PET

Holger Schirrmeister, Albrecht Guhlmann, Klaus Elsner, Jörg Kotzerke, Gerhard Glatting, Marion Rentschler, Bernd Neumaier, Harald Träger, Karin Nüssle and Sven N. Reske

Departments of Nuclear Medicine and Diagnostic Radiology, University Hospital, Ulm, Germany

Radionuclide bone scanning (RNB) is considered to be the most practical screening technique for assessing the entire skeleton for skeletal metastases. However, RNB has been shown to be of lower sensitivity than MRI and CT in detecting osteolytic metastases. A prospective study was designed to evaluate the accuracy of planar RNB versus tomographic bone imaging with ^{18}F-labeled NaF and PET (^{18}F PET) in detecting osteolytic and osteoblastic metastases and its dependency on their anatomic localization. **Methods:** Forty-four patients with known prostate, lung or thyroid carcinoma were examined with both planar RNB and ^{18}F PET. A panel of reference methods including MRI of the spine, ^{131}I scintigraphy, conventional radiography and spiral CT was used as the gold standard. RNB and ^{18}F PET were compared by a lesion-by-lesion analysis using a five-point score for receiver operating characteristic (ROC) curve analysis. **Results:** ^{18}F PET showed 96 metastases (67 of prostate carcinoma and 29 of lung or thyroid cancer), whereas RNB revealed 46 metastases (33 of prostate carcinoma and 13 of lung or thyroid cancer). All lesions found with RNB were also detected with ^{18}F PET. Compared with ^{18}F PET and the reference methods, RNB had a sensitivity of 82.8% in detecting malignant and benign osseous lesions in the skull, thorax and extremities and a sensitivity of 40% in the spine and pelvis. The area under the ROC curve was 0.99 for ^{18}F PET and 0.64 for RNB. **Conclusion:** ^{18}F PET is more sensitive than RNB in detecting osseous lesions. With RNB, sensitivity in detecting osseous metastases is highly dependent on anatomic localization of these lesions, whereas detection rates of osteoblastic and osteolytic metastases are similar. Higher detection rates and more accurate differentiation between benign and malignant lesions with ^{18}F PET suggest the use of ^{18}F PET when possible.

Key Words: ^{18}F PET; radionuclide bone scanning; bone metastases

J Nucl Med 1999; 40:1623–1629

Early detection of metastatic bone disease and definition of its extent, pattern and aggressiveness are important prerequisites for adequate treatment (*1*) by resection (*2*), radiation (*3*) or systemic therapy (*1,4,5*). Currently, screening for skeletal metastases is usually performed with planar radionuclide bone scintigraphy (RNB) even though tomographic imaging modalities such as MRI and CT have been shown to be superior to planar RNB (*6–10*). However, MRI and CT are impractical for routine whole-body screening for bone metastases.

In the past, planar scintigraphy with ^{18}F-labeled NaF has been considered less accurate than bone scanning with technetium-labeled phosphonates (*11,12*). Whether this finding was the result of different technical parameters or a different amount of tracer accumulation in malignant lesions remained unclear. More accurate bone scanning should be feasible with the higher detection efficiency and superior spatial resolution of PET scanners in comparison with standard gamma camera systems. We devised a prospective study of patients with malignant solid tumors to compare the diagnostic accuracy of 1-h routine ^{18}F PET scanning of the skeletal trunk with the diagnostic accuracy of conventional bone scintigraphy. Because planar RNB is currently the method of choice for routine skeletal surveys, PET was tested against planar imaging. Sensitivities in the detection of benign and malignant lesions were compared in different regions of the skeleton. We selected patients with cancer of the prostate to examine the sensitivity of these methods in detecting mainly osteoblastic metastases. Patients with lung cancer or thyroid cancer were recruited to evaluate the ability of these methods to detect mainly osteolytic metastases.

MATERIALS AND METHODS

Patient Selection

Between March 1996 and August 1997 we recruited 44 patients with known (9 patients) or suspected (35 patients) bone metastases from cancer of the prostate (20 patients), the lung (5 patients) or the thyroid (19 patients). Malignant disease was histologically proven in all patients. Only patients with clinical stage III or IV disease were selected. Pregnant patients and patients with previously known disseminated metastatic bone disease (5 bone metastases), medullary or anaplastic thyroid cancer or unknown clinical stage or clinical stage I or II disease were excluded from the study. All patients were prospectively examined with ^{18}F PET and RNB.

Diagnosis of detectable lesions was proven by MRI, spiral CT,

Received Oct. 13, 1998; revision accepted Mar. 12, 1999.

For correspondence or reprints contact: Sven N. Reske, MD, Department of Nuclear Medicine, University of Ulm, Robert Koch Str. 8, D-89070 Ulm, Germany.

whole-body ^{131}I scintigraphy, ^{18}F-fluorodeoxyglucose (FDG) PET or radiography (reference methods are summarized in Table 1). MRI (30 patients) or spiral CT (12 patients) of the vertebral column was prospectively performed in 41 patients. All patients gave informed consent to participate in this study, which was approved by the local ethical commission of the University of Ulm.

^{18}F PET Imaging

One hour after intravenous injection of 370 MBq ^{18}F-labeled NaF, data acquisition with a high-resolution PET scanner (ECAT EXACT HR$^+$; CTI/Siemens, Inc., Knoxville, TN; full width at half maximum [FWHM] 4.2–5.5 mm, axial field of view 15.5 cm, no attenuation correction) was started. Acquisition time was 10–12 min per bed position (seven bed positions per patient). The scans routinely covered the skull, upper extremity, thorax, pelvis and proximal femur in all patients. The lower leg was not examined with PET in this series because metastases located in the lower leg are very uncommon. Transmission scanning was not performed for the purpose of shorter and more practical examination times. Coronal, transverse and sagittal sections of 4.5-mm thickness and projection images were routinely reviewed in hard-copy form in a standardized manner.

Radionuclide Bone Scanning

For standard bone scans a double-head gamma camera (Bodyscan; Siemens, Erlangen, Germany; FWHM 4.9–7.9 mm, field of view 50 cm, low-energy high-resolution collimator, 1024 × 256 matrix) was used. Three hours after injection of 740 MBq ^{99m}Tc-methylene diphosphonate, data acquisition with 1.5 million counts per head was begun.

MRI Protocol

In 30 patients, MRI examinations of three vertebral regions (cervical, thoracic and lumbar spine) were performed (Table 1). Each region was imaged in two perpendicular planes with a T1-weighted spinecho sequence (body array, repetition time [TR] 532 ms, echo time [TE] 15 ms, 15.5-mm slices, gap 0.5 mm) and a fat-suppressed T2-weighted sequence (turbo inversion recovery, TR 6004 ms, TE 60 ms, inversion time 140 ms, flip angle 180, 140.5-mm slices, gap 0.5 mm). If a patient had 5 lesions, one of the spinecho sequences was repeated after intravenous application of 0.2 mmol/kg body weight gadolinium (Magnevist; Schering, Berling, Germany) to verify typical contrast enhancement of metastasis.

Additional Imaging Modalities

Spiral CT was performed in 12 patients to estimate fracture risk of suspected vertebral metastases detected by RNB or ^{18}F PET (Table 1). CT scanning was also performed in these patients at normal vertebral regions to exclude additional vertebral metastases. MRI was not performed in 11 of the patients who underwent spiral CT of the entire vertebral column. Whole-body ^{131}I scintigraphy was performed in all 19 patients with thyroid cancer. Five patients had additional FDG PET to exclude iodine-negative metastases. FDG PET was also performed in 1 patient with lung cancer. A clinical follow-up period of at least 1 y was used as the gold standard in 3 patients with normal RNB and ^{18}F PET who refused MRI of the spine (Table 1).

Interpretation of Radionuclide Bone Scanning and ^{18}F PET

Lesions were classified as degenerative if they were located at joints. Rib lesions were regarded as traumatic when adjacent lesions in the ribs occurred or when the rib lesions were located at the costochondral joints. Characteristic linear tracer accumulation of a fractured endplate or extravertebral location of osteophytes was also defined as benign. All lesions not showing characteristic features of fractures or degenerative disease were defined as metastases.

TABLE 1
Reference Methods

Reference methods	Patients: No.	No. with additional FDG PET	No. with additional radiography
MRI, spiral CT	1	1	—
MRI	19	—	6
MRI, whole-body ^{131}I scan	10	3	5
Spiral CT	7	2	4
Spiral CT, whole-body ^{131}I scan	4	1	2
1-y follow-up	3	—	—

FDG = ^{18}F-fluorodeoxyglucose.

Interpretation of Reference Methods

Patients were classified as having no bone metastases when MRI of the spine, whole-body iodine scintigraphy and additional imaging methods showed no sign of osseous metastases or when lesions detected by RNB or ^{18}F PET were not proven to be metastatic by the reference methods.

Lesions were defined as metastatic when ^{131}I accumulation on whole-body iodine scintigraphy or typical gadolinium enhancement on T1-weighted and hyperintense lesions on fat-suppressed T2-weighted MRI was present. The osteolytic appearance on CT or radiography of suspected lesions detected with ^{18}F PET or RNB was also used as a criterion for osseous metastases. Focal FDG skeletal accumulation on whole-body FDG PET was another criterion for confirmation of the diagnosis of bone metastases.

Interpretation of ^{18}F PET in Disseminated Metastatic Bone Disease

Disseminated metastatic bone disease was found in 2 patients with prostate cancer. One of these patients had two previously known metastases, whereas metastatic bone disease was previously unknown in the other patient. Because identification and separate assessment of all lesions were impractical, the interpretation of MRI and ^{18}F PET was modified. When multiple lesions were found in one vertebral body or rib, they were defined as one single metastatic lesion. Only the vertebral lesions were verified by the reference methods in these 2 patients. The rib lesions were also defined as metastases, although they were not verified by reference methods.

Data Analysis

Experienced nuclear medicine physicians independently interpreted RNB or ^{18}F PET. All reviewers were unaware of the results of the reference methods. Two diagnostic radiologists reviewed each MR image, spiral CT scan, whole-body iodine scintigram and radiograph. The reviewers of MR images or spiral CT scans were provided with the additional reference methods but were unaware of the results of ^{18}F PET or RNB. Discrepant interpretations of the two readers were resolved by consensus.

^{18}F PET and RNB were compared by a lesion-by-lesion analysis.

In 42 patients, every lesion was judged on a five-point scale as metastasis (score 1), probably metastasis (score 2), equivocal (score 3), probably benign (score 4) or benign (score 5). Lesions on ^{18}F PET that were not visible on RNB were defined as benign on RNB. A modified five-point scale was used for 2 patients with disseminated metastatic bone disease. Receiver operating characteristic (ROC) curve analysis was performed, and the area under the curve was used to test for statistically significant differences between both imaging modalities (*13*). A P of 0.05 was considered statistically significant.

RESULTS

Differences Between Radionuclide Bone Scanning and ^{18}F PET in Skeletal Staging

The reference methods indicated that 15 of the 44 patients had osseous metastases. All 15 patients were identified as having metastases by ^{18}F PET and only 13 (9 of 9 with previously known metastatic bone disease and 4 of 6 without previously known metastatic bone disease) by RNB. ^{18}F PET correctly staged the extent of metastatic bone disease in comparison with the reference methods. RNB detected all metastatic lesions in only 7 of 15 patients. Additional metastases were seen in the remaining 8 patients using the reference methods. Benign lesions were detected in 29 patients with ^{18}F PET and in only 20 patients with RNB (Table 2).

Lesion-by-Lesion Analysis

With ^{18}F PET, 205 lesions were detected, of which 96 were associated with metastases and 109 were not metastatic. With RNB, 42 metastases and 66 benign lesions were detected (Table 3). Compared with ^{18}F PET, RNB was clearly less sensitive in detecting both osteoblastic and osteolytic metastases and in detecting benign lesions (Table 4).

Both RNB and ^{18}F PET revealed 108 lesions. With ^{18}F PET, 105 lesions (97.2%) were correctly classified as metastases (n = 45) or benign (n = 60). One benign lesion was misclassified as metastasis. One benign lesion and one metastasis were classified as equivocal. We interpreted 87 lesions (80.5%) correctly with RNB. Six metastases and 7 benign lesions were classified as equivocal. Eight lesions, of which 3 were benign and 5 were metastatic, were misclassified. We found 97 lesions with ^{18}F PET that were not visible on RNB. Of these lesions, 94 (96.9%) were judged correctly as metastases (n = 44) or as benign (n = 50). Three benign lesions were classified as equivocal. Compared with ^{18}F PET and the reference methods, RNB had a sensitivity in detecting benign and malignant lesions of 79.2%–88.9% in the skull, thorax (ribs and sternum) and extremities and of 20.5%–43.2% in the spine and pelvis (Table 5).

Two patients with prostate cancer had disseminated metastatic bone disease. Forty-three of the 67 osteoblastic metastases detected with ^{18}F PET and 11 of the 33 metastases detected with RNB were observed in these 2 patients. One patient with thyroid cancer had 8 osseous metastases and an additional 12 patients had between 1 and 5 metastases.

Based on lesion-by-lesion analysis, ^{18}F PET showed significantly ($P < 0.05$) superior results in the detection of benign and malignant lesions of the skeleton. The area under the ROC curve was 0.99 for ^{18}F PET and 0.64 for RNB.

TABLE 2
Patients with Metastases, Benign Lesions or Normal Findings on Radionuclide Bone Scanning (RNB) or PET

	Patients with metastases	Extent of metastases correct	Patients with benign lesions	Patients with normal findings
^{18}F PET	15	15	29	8
RNB	13*	7	20	17
Reference methods	15	15	29	8

*Malignant lesions, including 2 patients with metastases that were misinterpreted as probably benign or equivocal.

Eight patients with bone metastases had additional benign findings.

TABLE 3
Benign and Malignant Lesions Detected by Radionuclide Bone Scanning (RNB) and ^{18}F PET

Lesions	^{18}F PET	RNB
Benign	109	66
Metastases	96	42
Total	205	108

DISCUSSION

With ^{18}F PET twofold more lesions were detected than with RNB. The detection rates of bone metastases were 100% with PET both in patients with osteoblastic metastases associated with cancer of the prostate and in patients with osteolytic metastases associated with cancer of the thyroid or lung. In contrast, with RNB only 49.3% of the osteoblastic metastases and 44.8% of the osteolytic metastases were detected. The detection rates of malignant and benign lesions were 40%–42% in the spine and pelvis and 80%–90% in the thorax, skull and extremities. Two patients were staged as false-negative with RNB, but no patient was staged as false-negative with ^{18}F PET.

^{18}F PET was correct in the diagnosis of 44 patients and RNB was correct in the diagnosis of 42 patients who were staged as M1 or M0 on bone site, whereas the extent of

TABLE 4
Skeletal Metastases Detected by ^{18}F PET and Radionuclide Bone Scanning (RNB) in Patients with Osteoblastic (Prostate Cancer) or Osteolytic (Lung and Thyroid Cancer) Metastases

Metastases	^{18}F PET	RNB	RNB/PET (%)
Osteoblastic	67	33	49.3
Osteolytic	29	13	44.8

TABLE 5
Osseous Lesions Detected at Different Sites by Radionuclide Bone Scanning (RNB) Compared with ^{18}F PET

Region	^{18}F PET	RNB*
Skull	5	4 (80.0)
Upper extremity	18	16 (88.9)
Ribs and sternum	24	19 (79.2)
Spine	135	55 (39.6)
Cervical	39	8 (20.5)
Thoracic	59	21 (33.6)
Lumbar	37	16 (43.2)
Pelvis	12	5 (41.7)
Lower extremity	11	9 (81.8)

*Values in parentheses indicate percentage of lesions detected by ^{18}F PET.

metastatic bone disease was underestimated in 8 patients by RNB and correctly diagnosed in all patients by ^{18}F PET (Table 2). Surgical treatment (*2*) or radiation therapy (*3*) is a suitable treatment modality for prolongation of survival of patients with isolated bone metastases. In contrast, systemic therapy (*1,4,5*) is appropriate in patients with widespread involvement of the skeleton. Therefore, correct description of the extent of metastatic bone disease is essential for selection of the optimal therapy.

Compared with RNB, ^{18}F PET showed higher accuracy in detecting both osteolytic and osteoblastic metastases (Table 4). No significant difference between the detection of osteoblastic and osteolytic metastases with RNB was found. The lesion-by-lesion analysis suggests that failure to detect osteolytic lesions with RNB, which is a frequently discussed problem, might be overcome with ^{18}F and PET. In comparison with RNB, ^{18}F PET had not only a much higher rate in

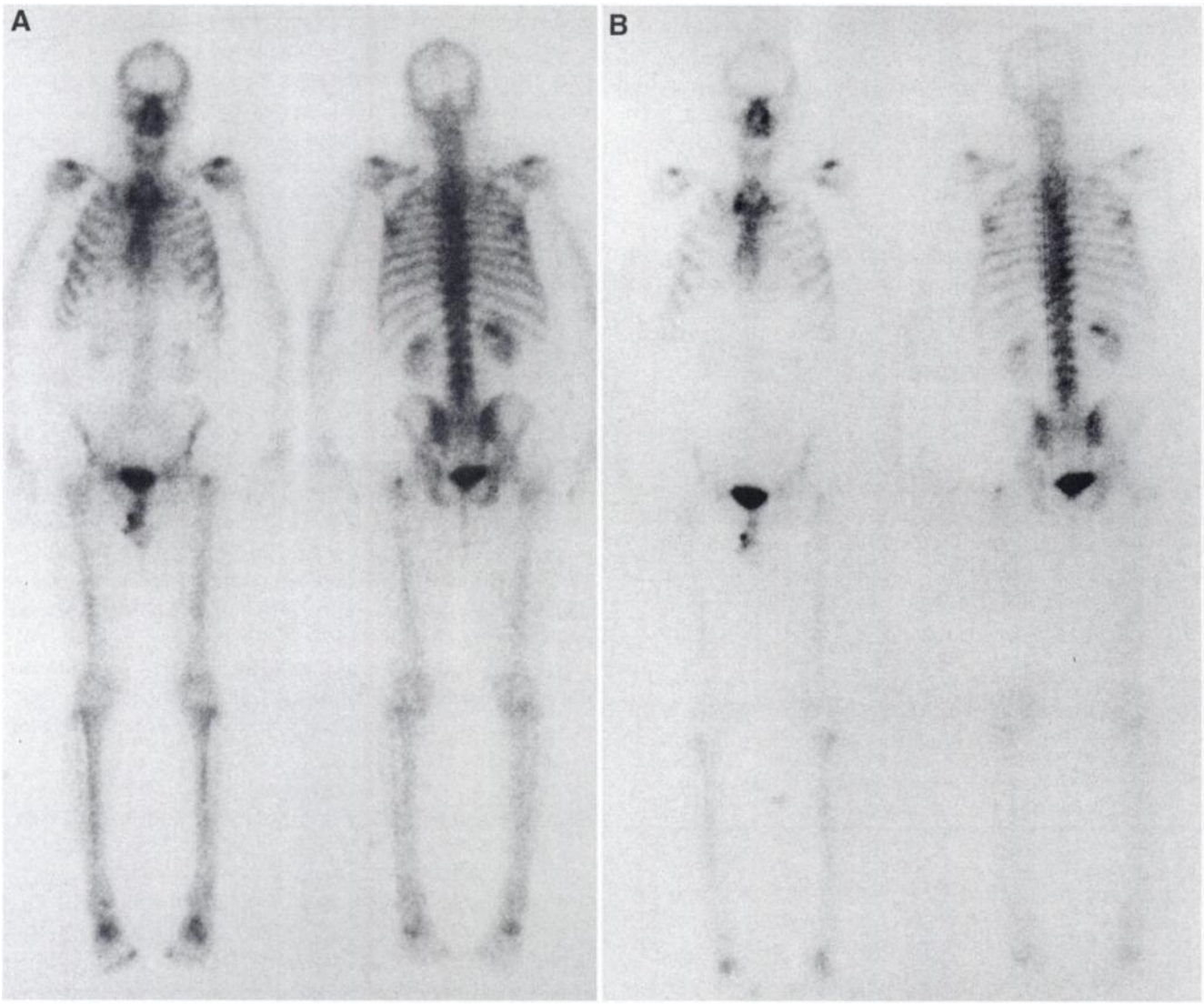

FIGURE 1. A 66-y-old man with prostate cancer. Planar bone scan (dual-intensity mode) shows metastases in proximal left femur (A) and in thoracic spine (B).

detecting skeletal lesions but also a higher accuracy in differentiating benign from malignant lesions.

In malignant solid tumors, the spine is the most common site of bone metastases (*14*). Furthermore, the spine is the first location of metastatic bone involvement in most patients with carcinoma of the prostate because the spread of tumor cells depends on the vertebral venous system (*15*). For this reason, imaging modalities with sufficient sensitivity for early diagnosis of vertebral metastatic bone disease are required. The sensitivity of RNB in detecting spinal lesions was as low as 20%–43% in our series. Higher sensitivities were obtained in the skull, thorax and extremities (Table 5). These results are in agreement with those of other studies (*6–10,16*) and might be related to relatively numerous small metastatic deposits in vertebral bodies not detected by low-resolution RNB.

Tomographic methods such as SPECT and PET allow detection of spinal lesions without superposition of soft tissue. Although SPECT is commonly used as a complementary method to differentiate between malignant and benign lesions (*14,17,18*) detected by planar scintigraphy, PET is primarily a tomographic method. The lower sensitivity in detecting spinal lesions with RNB might be improved by routine use of spinal SPECT.

^{18}F PET enables the detection of very small lesions before osteolytic destruction or osteoblastic osseous reaction is visible on RNB (Figs. 1–4). The current explanation that small lesions, which could be detected by MRI (*1*), bone marrow scintigraphy (*19*) or bone marrow biopsy (*10*), show no tracer accumulation on RNB is as follows: A temporal sequence in the metastatic process starts in the bone marrow and induces osteoblastic or osteolytic response of the osseous bone during further progression (*6–8,19–21*). In contrast, ^{18}F PET revealed a very early reaction of bone turnover in the metastatic process. Thus, the lower sensitivity of RNB in detecting these lesions might be related primarily to physical and pharmacologic imaging parameters (*22–24*) rather than to the pathophysiology of metastatic bone interaction.

Although patients with previously known disseminated metastatic bone disease were excluded from the study, 2 patients with prostate cancer had disseminated metastatic bone disease. The higher number of detected lesions in prostate cancer patients compared with the lower number of metastases in patients with lung or thyroid cancer is obviously associated with the 43 metastases detected by ^{18}F PET and the 11 metastases detected by RNB in the 2 prostate cancer patients with disseminated metastatic bone disease and not associated with a generally lower sensitivity in detecting osteolytic bone metastases with both imaging methods.

Single or double hot spots without known degenerative disease or trauma are present in approximately 14% of all RNB performed on patients with malignant tumors (*25*). Because of the low specificity of RNB, further examinations such as radiography, CT or MRI are necessary in these patients. This will impose physical strain and distress to patients and result in additional cost (*25*). Because of the superior spatial resolution of PET camera systems, ^{18}F PET scans offer more anatomic detail compared with conventional RNB (*26*). Superior anatomic localization of bone lesions (e.g., vertebral body versus intervertebral articulation) with ^{18}F PET is probably related to a superior specificity compared with RNB. In contrast to a diagnostically unclear situation with RNB, the diagnosis of metastatic bone disease is obvious in patients when disseminated metastatic bone disease is present on ^{18}F PET scans, even when exact anatomic localization is difficult (Figs. 1–4).

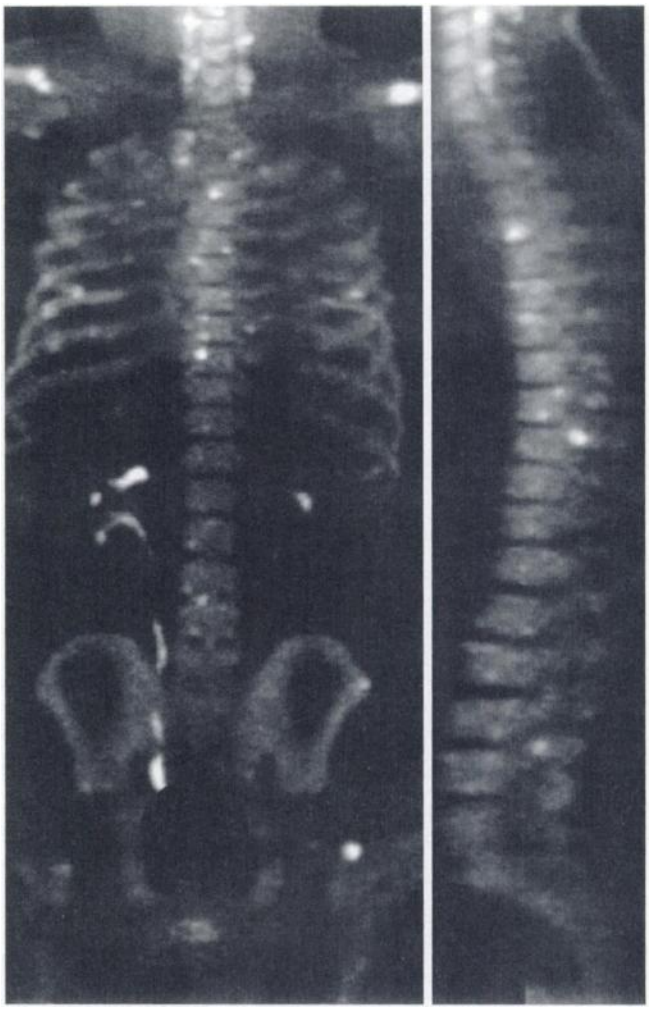

FIGURE 2. ^{18}F PET (same patient as in Fig. 1), maximal intensity projections: anterior view (left) and sagittal section (right). Focus is on thorax and vertebral column for better visualization of small lesions. Note disseminated metastatic bone disease of central skeleton and very small, low-intensity spots in lumbar spine corresponding to bone metastases.

One drawback of this study is that no imaging modality currently exists that can be used as a reference method to assess the entire skeleton. The detection rates of extravertebral osseous lesions by RNB were dependent on the results of ^{18}F PET because only visible lesions were corroborated by the reference methods. The vertebral column was the

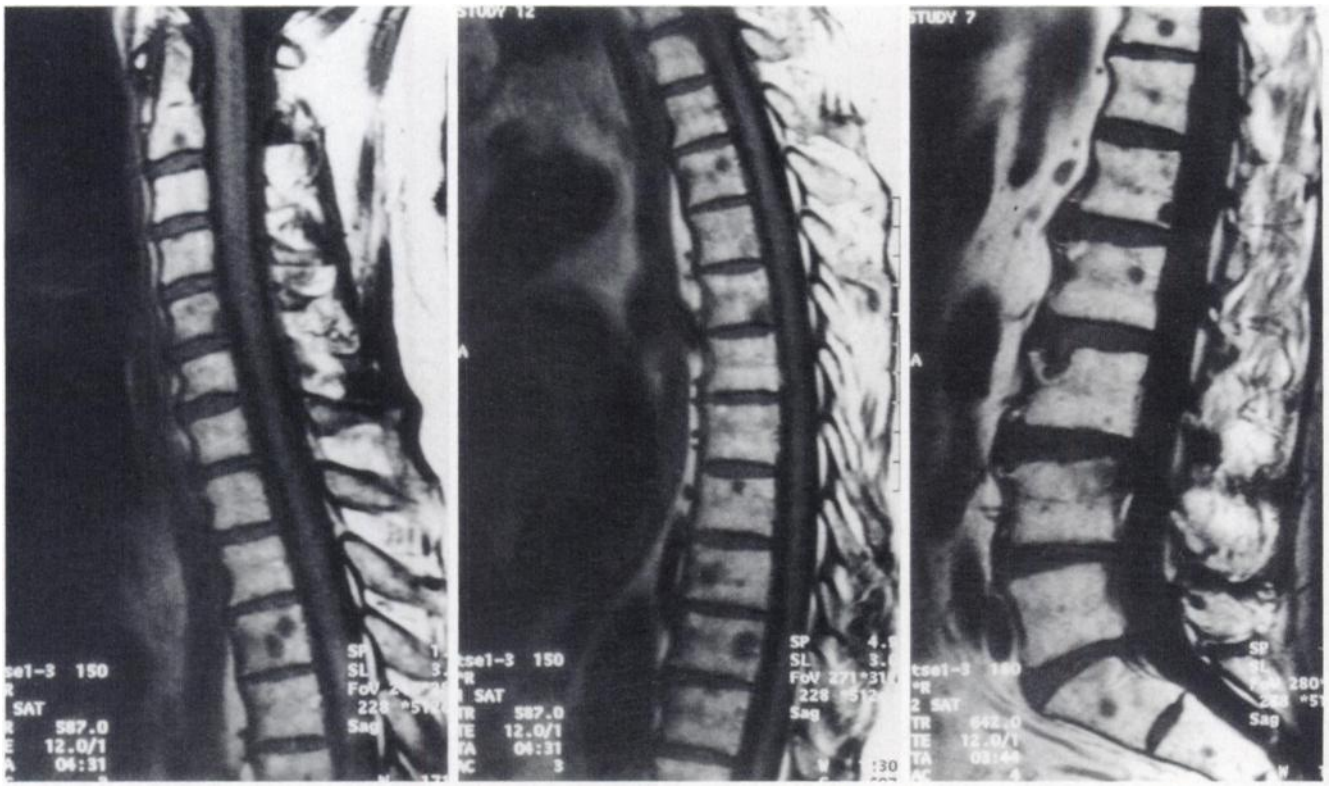

FIGURE 3. MR images of vertebral column. T1-weighted sagittal images of cervical (left), thoracic (center) and lumbar (right) spine show multiple vertebral lesions in patient shown in Figures 1 and 2.

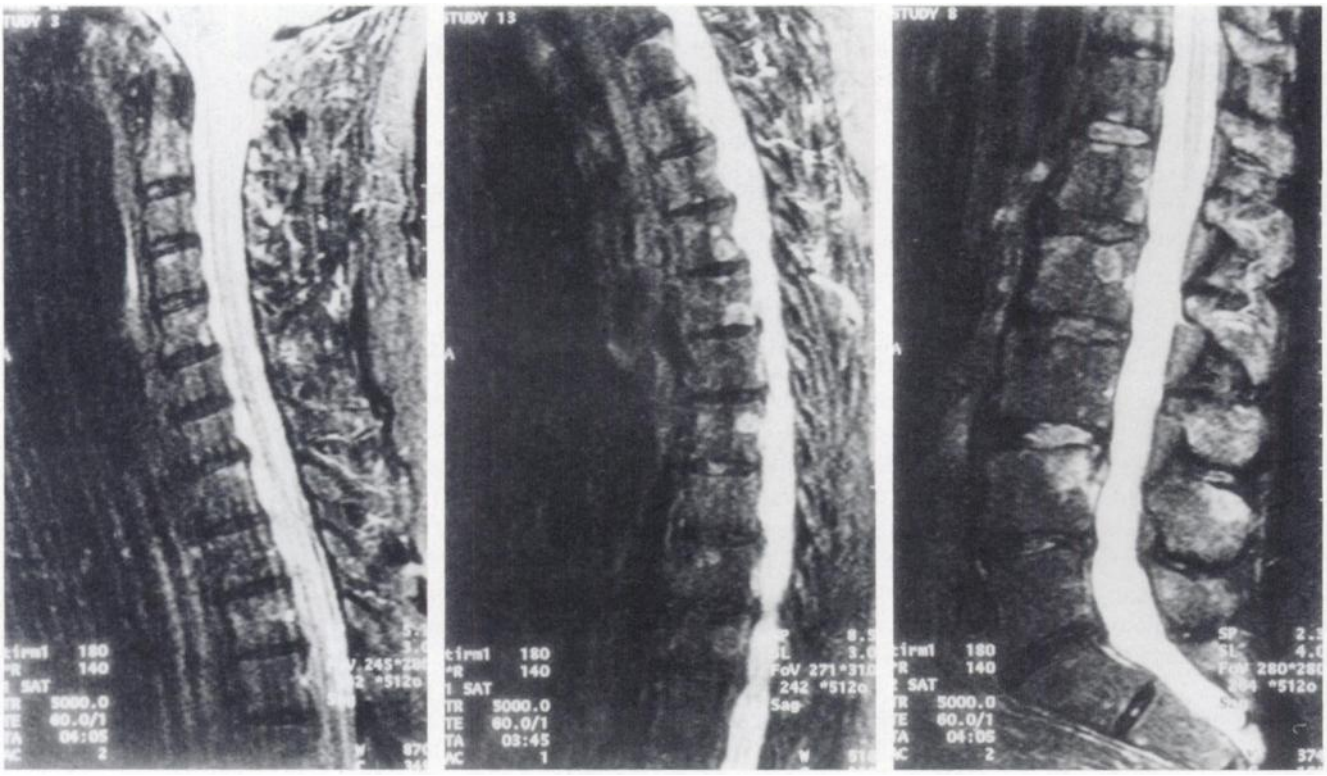

FIGURE 4. Fat-suppressed T2-weighted sagittal images of cervical (left), thoracic (center) and lumbar (right) spine show multiple hyperintense lesions associated with bone metastases. In contrast, Schmorl's node at ventral superior endplate of L3 shows no hyperintense signal.

only skeletal region that was prospectively examined in 41 of our patients. Because of the lack of a highly sensitive whole-body imaging modality, false-negative lesions located extravertebrally and not detected by PET or RNB could not be excluded by the reference methods. Another difficulty in interpreting the results of this study is the lack of histologic proof of the 205 lesions detected with ^{18}F PET. However, obtaining histologic proof of all skeletal lesions is impractical and is unethical when there is no impact on clinical management. Therefore, findings of noninvasive imaging modalities were not rigorously verified by histologic examination. Unless a large number of these lesions are pathologically confirmed, the conclusion that ^{18}F PET is more accurate than RNB may be premature. For this reason, the ROC curve analysis must be interpreted with caution. An area under the ROC curve of 0.99 for ^{18}F PET allows the conclusion that the accuracy of ^{18}F PET in detecting spinal lesions is very close to the accuracy of the MRI and spiral CT reference methods and is significantly ($P < 0.05$) higher than the accuracy of RNB (area under the ROC curve = 0.64).

CONCLUSION

Bone imaging with ^{18}F PET is clearly more sensitive than planar RNB in the detection of benign and malignant osseous lesions. The sensitivity in detecting benign and malignant bone lesions with RNB is highly dependent on their anatomic localization and independent thereof with ^{18}F PET. In this series, ^{18}F PET was as accurate as a panel of reference methods including MRI and CT. At present, ^{18}F PET remains time-consuming and probably is not cost-effective. Therefore, ^{18}F PET might be used at present in selected clinical situations in which findings of RNB complemented by SPECT are inconclusive. Based on the encouraging results of Kosuda et al. (*16*), further comparison of SPECT with ^{18}F PET is needed before a definite conclusion on the routine use of ^{18}F PET can be made.

ACKNOWLEGMENTS

The authors thank Dr. Christoph Diederichs for helpful suggestions and Jennifer Ziedler for editing and reviewing the manuscript.

REFERENCES

1. Coleman RE, Rubens RD. The clinical course of bone metastases from breast cancer. *Br J Cancer*. 1987;55:61–66.
2. Noguchi S, Miyauchi K, Nishizawa Y, Imaoka S, Koyama H, Iwanaga T. Results of surgical treatment for sternal metastasis of breast cancer. *Cancer*. 1988;62:1397–1401.
3. Needham PR, Hoskin PJ. Radiotherapy of painful bone metastases. *Palliat Med*. 1994;8:95–104.
4. van Holten-Verzahntvoort AT, Bijvoet OL, Cleton FJ, et al. Reduced morbidity from skeletal metastases in breast cancer patients during long-term biphosphonate-treatment. *Lancet*. 1987;31:983–985.
5. Sasaki A, Boyce BF, Story B, et al. Bisphosphonate residronate reduces metastatic human breast cancer burden in bone in nude mice. *Cancer Res*. 1995;55:3551–3557.
6. Traill Z, Richards MA, Moore NR. Magnetic resonance imaging of metastatic bone disease. *Clin Orthop*. 1995;312:76–88.
7. Franks JA, Ling A, Patronas NJ, et al. Detection of malignant bone tumors: MR imaging vs scintigraphy. *AJR*. 1990;155:1043–1048.
8. Brown B, Laorr A, Greenspan A, Stadalnik R. Negative bone scintigraphy with diffuse osteoblastic breast carcinoma metastases. *Clin Nucl Med*. 1994;19:194–196.
9. Haubold-Reuter, Duewell S, Schilcher Marincek B, Schulthess GK. The value of bone scintigraphy, bone marrow scintigraphy and fast spin magnetic resonance imaging in staging of patients with malignant solid tumors: a prospective study. *Eur J Nucl Med*. 1993;20:1063–1069.
10. Avrami E, Tadmor R, Dally O, Hadar H. Early MR demonstration of spinal metastases in patients with normal radiographs and CT and radionuclide bone scans. *J Comput Assist Tomogr*. 1989;13:598–602.
11. Silberstein EB, Saenger EL, Tofe AJ, Alexander GW, Park HM. Imaging of bone metastases with ^{99m}Tc-Sn-EHDP (diphosphonate), ^{18}F, and skeletal scintigraphy. *Radiology*. 1973;107:551–555.
12. Weber DA, Keyes JW, Landman S, Wilson GA. Comparison of Tc^{99m} polyphosphonate and ^{18}F for bone imaging. *AJR*. 1974;121:184–190.
13. Hanley JA, McNeil BJ. A method of comparing the areas under receiver operating characterisitic curves from the same cases. *Radiology*. 1983;148:839–843.
14. Krasnow AZ, Hellman RS, Timins ME, Collier BD, Anderson T, Isitman AT. Diagnostic bone scanning in oncology. *Semin Nucl Med*. 1997;27:107–141.
15. Batson OV. The function of the vertebral veins and their role in the spread of metastases. *Clin Orthop*. 1995;312:4–9.
16. Kosuda S, Tatsumi K, Yokoyama H, et al. Does bone SPECT actually have lower sensitivity for detecting vertebral metastases than MRI? *J Nucl Med*. 1996;37:975–978.
17. Even-Sapir E, Martin RH, Barnes DC, Pringle CR, Iles SE, Mitchell MJ. Role of SPECT in differentiating malignant from benign lesions in the lower thoracic and lumbar vertebrae. *Radiology*. 1993;187:193–198.
18. Donhoe KJ, Henkin RE, Royal HD, et al. Procedure guideline for bone scintigraphy: 1.0. *J Nucl Med*. 1996;37:1903–1906.
19. Reske SN, Karstens JH, Gloeckner W, et al. Radioimmunoimaging for diagnosis of bone marrow involvement in breast cancer and malignant lymphoma. *Lancet*. 1989;11:299–301.
20. Pantel K, Izbicki J, Passlick B, et al. Frequency and prognostic significance of isolated tumor cells in bone marrow of patients with non-small-cell lung cancer without overt metastases. *Lancet*. 1996;347:649–653.
21. Kamby C, Vejeborg I, Daugaard S, et al. Clinical and radiologic characteristics of bone metastases in breast cancer. *Cancer*. 1987;60:2524–2531.
22. Hoh CK, Hawkins RA, Dahlborn M, et al. Whole body skeletal imaging with ^{18}F-ion and PET. *J Comput Assist Tomogr*. 1993;17:34–41.
23. Hawkins RA, Choi Y, Huang SC, et al. Evaluation of skeletal kinetics of fluorine 18-fluoride ion with PET. *J Nucl Med*. 1992;33:633–642.
24. Schiepers C, Nuyts J, Bormans G, et al. Fluoride kinetics of the axial skeleton measured in vivo with fluorine-18-fluoride PET. *J Nucl Med*. 1997;38:1970–1976.
25. Puig S, Staudenherz A, Steiner S, Eisenhuber E, Leitha T. Differential diagnosis of atypically located single or double hot spots in whole body scanning. *J Nucl Med*. 1998;39:1263–1266.
26. Schirrmeister H, Rentschler M, Kotzerke J, Diederichs CG, Reske SN. Skeletal imaging with ^{18}FNa-PET and comparison with planar skeletal scintigraphy. *Fortschr Röntgenstr*. 1998;168:451–456.